

97.4%-Efficient All-GaN Dual-Active-Bridge Converter with High Step-up High-Frequency Matrix Transformer

Armin Jafari, Mohammad Samizadeh Nikoo, Furkan Karakaya, Nirmana Perera and Elisa Matioli

Power and Wide-band-gap Electronics Research Laboratory (POWERlab),
École polytechnique fédérale de Lausanne (EPFL), CH-1015 Lausanne, Switzerland

Corresponding author: Armin Jafari, armin.jafari@epfl.ch

Abstract

In this work, we demonstrate a state-of-the-art high step-up/down dual-active-bridge (DAB) converter designed with GaN transistors, to achieve a high efficiency and large power-density. A quasi-planar matrix transformer with high step-up/down ratio is demonstrated, whose leakage inductance is responsible for achieving soft-switching and power-transfer, without using any external inductors, resulting in a compact converter. A combination of low-voltage (LV) and high-voltage (HV) GaN transistors operating at both primary and secondary bridges, enabled operation at 300 kHz to significantly reduce the size of the ferrite core in the transformer. By applying the simplest modulation (single phase shift) suitable for very high switching frequencies, the converter could transfer up to 500 W (reaching up to 10 kW/l or 164 W/inch³ in power-density) with a peak efficiency of 97.4% at a 12-time step-up. After discussing guidelines of passive and active component design and selection, we benchmark DC-DC converters and compare the performance of our design to other state-of-the-art high-frequency converters. Furthermore, we discuss how such DC/DC converters could serve as chargers in electric vehicles (EVs) to provide efficient power transfer in a compact size with galvanic isolation, which is required for such applications. The converter can be regarded as a flexible DC transformer in future DC distribution systems and microgrids for efficient, compact and regulated power transfer.

1 Introduction

Dual-active-bridge (DAB) topology has bidirectional power-transfer capability and, due to straightforward regulation of voltage and power, is widely used in medium and high-voltage DC power systems [1]. Many power electronics systems at low-voltage such as battery chargers for electric vehicles, telecommunications, avionics, wind and solar generation systems and in specific DC microgrids in distribution level could benefit from DAB topology [2]. The required step-up/down is provided by the turns ratio of the employed transformer and the power is regulated by the phase-shift between the voltages generated by primary and secondary full-bridges (see Fig. 1). Power-transfer in DAB is inductive [3] and the high switching frequency of GaN transistors leads to a significant reduction in the transformer size [4], [5] and thus a high power density. Soft-switching capability of DAB, low device ON-resistance and small gate and output capacitance (C_{OSS}) losses in GaN transistors at frequencies around 1 MHz (most ferrites operate at this frequency range),

enable design of high-efficiency DABs for low-voltage power conversion based on wide-band-gap (WBG) transistors [6], [7]. Several methods are employed to improve the light-load and high-voltage-gain efficiency of DAB topology even further, including alternative modulation schemes [3], [8], [9], addition of extra resonant components [10], [11] and using DAB in a composite converter [12]. Our proposed enhanced-DAB (E-DAB) topology employs only a tapped high-frequency (HF) transformer to boost efficiency without complicated modulations and adds no extra lossy components to the topology [4].

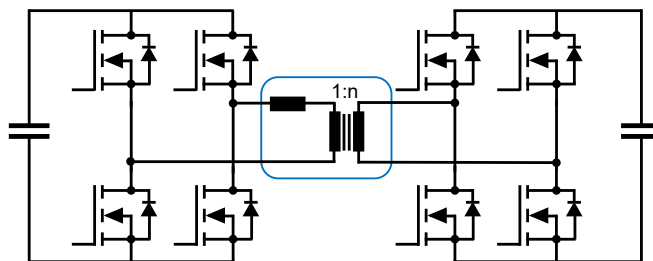


Fig. 1 DAB converter with a transformer at its core resembles a regulated DC transformer.

This work was supported in part by the Swiss Office of Energy under Grant SI/501887-01 (MEPCO).

In this paper, we discuss the design guidelines, experimental results and recommended applications of the HF DAB. In section 2, we introduce a novel quasi-planar matrix transformer for voltage step up/down where the resonance between its leakage inductance and capacitance of the field-effect transistors (FETs) leads to zero-voltage switching (ZVS), enabling efficient operation of the converter at a high frequency of 300 kHz. We further provide electrical measurements and magnetic finite-element analysis (FEA) results, required for design and evaluation of such HF transformer. Section 3 discusses a selection criterion for WBG FETs for achieving ZVS in DAB. In section 4, the overall circuit design is presented in details. Section 5 discusses experimental results and the performance of the converter at high frequency for different load conditions, with inclusion of a benchmarking for state-of-the-art DC-DC converters. In section 6 we introduce the gain versus power-transfer characteristic of the DAB converter, which is of great significance to control strategy for efficient power transfer in applications such as electric vehicle (EV) battery charging. We highlight the achievements in conclusion.

2 Design of High-frequency Matrix Transformer

Proper design of the transformer is crucial, as it is responsible for achieving high step-up/down, galvanic isolation between primary and secondary, and its leakage inductance enables soft-switching. For this purpose, we designed a quasi-planar matrix transformer (Fig. 2a) whose leakage inductance (L_r) and small AC resistance (R_{AC}) is measured in Fig. 2b using E4990A impedance analyzer. The windings consist of Litz wires (1050/#42 for primary and 66/#42 for secondary), which significantly reduces R_{AC} , to increase the efficiency at high currents. To optimize the size and shape of the ferrite cores, FEA (COMSOL) was used to evaluate the magnetic flux density inside the cores. An array of four toroidal cores (R22.1x13.7x7.9 N49 ferrite material) were used in a quasi-planar geometry to achieve the highest power-density. FEA analysis of magnetic flux density (B) for short-circuit and no-load conditions are shown in Fig. 3a, b. B tends to be very small when the load is high, and therefore the transformer core loss is almost negligible at heavy loads, where R_{AC} (winding loss) becomes important. On the other hand, at light loads, B becomes large and core loss becomes dominant.

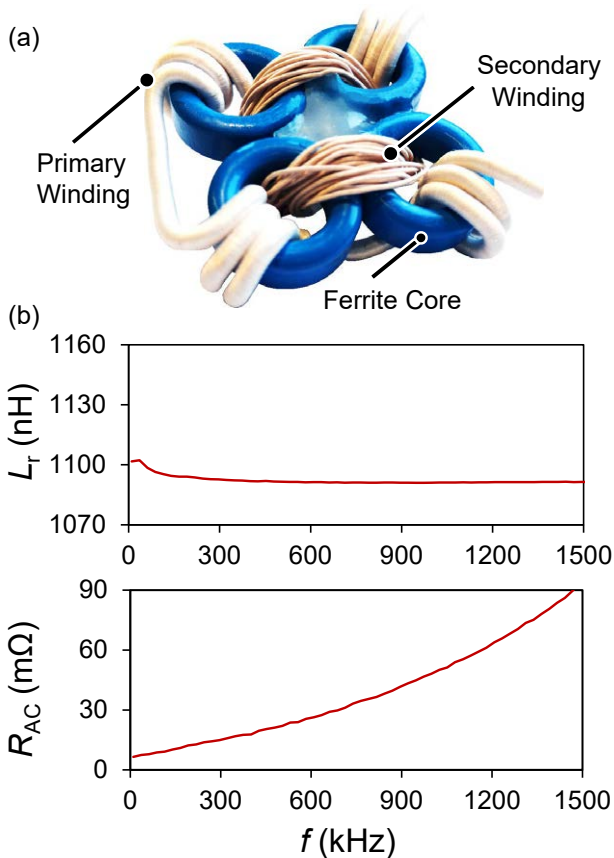


Fig. 2 (a) Quasi-planar HF matrix transformer with its (b) short-circuit parameters (L_r and R_{AC}) versus frequency, measured using E4990A impedance analyzer and the 16047E test fixture.

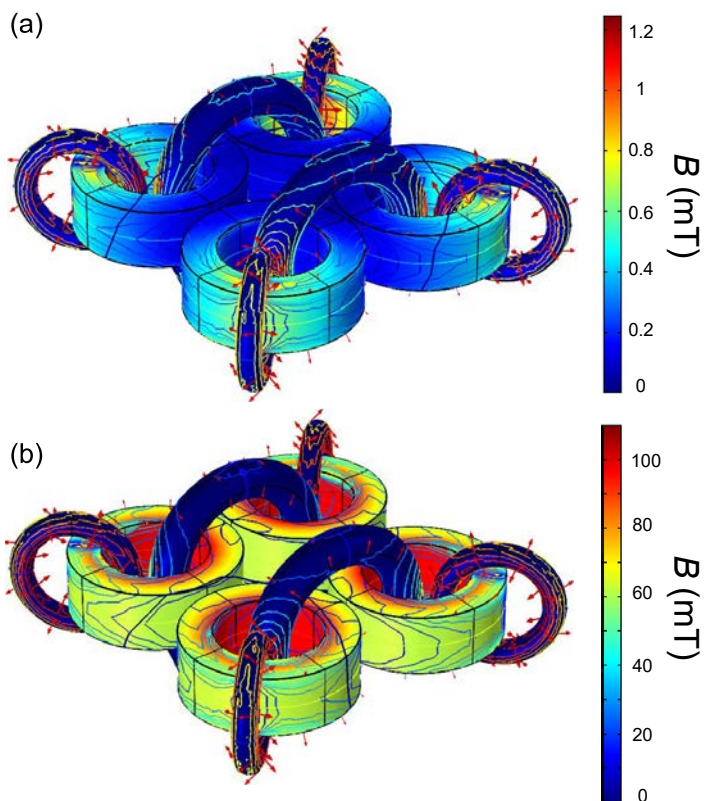


Fig. 3 FEA results for magnetic flux density (B) in HF matrix transformer under (a) short-circuit and (b) no-load conditions (40-V primary voltage at 300 kHz). Evaluation of B gives the core loss.

We decided to use toroidal shape, as it provides the most uniform magnetic flux distribution inside the core (Fig. 3b) compared to other geometries which have rectangular, sharp edges. FEA analysis allows the designer to address the trade-off between core area and switching frequency to minimize core loss, as [5]

$$B_{Peak} = \frac{V_{Peak}}{4fnA_{Min}} \quad (1)$$

where B_{PEAK} is the peak magnetic flux density, V_{Peak} is the voltage peak, f is the applied switching frequency, A_{Min} is the minimum core cross section and n is the turns ratio (here $n = 12$). Analysis based on FEA and (1) determine the loss behavior at light loads, where flux cancellation does not occur in the core, and large B leads to excessive core loss.

3 Selection of GaN FETs

Appropriately selected switches guarantee soft-switching and a high efficiency at the target operating point. For this design, we intended to design a converter with an input voltage in the range of 20 V to 40 V (at the primary side) and output voltage of 400 V (at the secondary side). The primary voltage is compatible with standard commercial photovoltaic (PV) panels and the output voltage is becoming the standard DC-link voltage for many applications such as EV batteries and DC distribution networks.

ON resistance ($R_{DS(ON)}$) in transistors increases as the output capacitance becomes smaller, and one requires a criterion to select the switches based on the trade-off between conduction loss and losses due to losing soft-switching. The DAB is a quasi-resonant converter, and one can use the energy balance during the resonance to select the switches. Peak energy stored in the inductor, L_r , can be formulated as

$$E_L = \frac{1}{2} L_r I^2 \quad (2)$$

where I is the peak inductor current. This energy should be large enough to charge and discharge the output capacitance of switches in each full-bridge. The required energy to charge or discharge the C_{OSS} between 0 to V for each transistor is

$$E_C = \frac{1}{2} C_{OSS} V^2 \quad (3)$$

Where C_{OSS} is the energy-related output capacitance of the transistor. During each resonance, two capacitors get charged and two

get discharged. By comparing the energy values from (2) and (3), one can estimate the minimum inductor current (and equivalently power) at which a transistor can be soft-switched in primary and secondary full-bridges. Low-voltage (LV) EPC transistor (EPC2031, EPC2032 and EPC2033) are compared in Fig. 4 for their output capacitance versus the minimum required primary current ($I_{PRIMARY}$) for soft-switching. For current values above 3 A, all the three transistors can achieve ZVS. As the converter is high power and the nominal $I_{PRIMARY}$ is in the order of 10 A, we decided to select the EPC2031 with the lowest $R_{DS(ON)}$ to reduce conduction losses. Similar comparison is performed for high-voltage (HV) transistors from GaN Systems, as shown in Fig. 5.

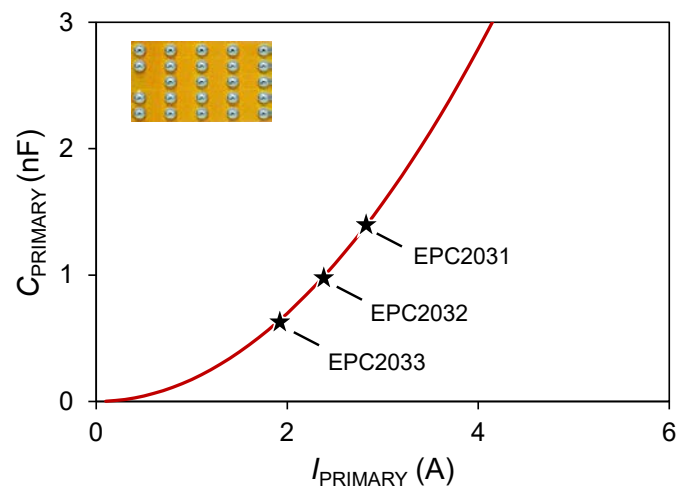


Fig. 4 For selecting LV transistors, since nominal $I_{Primary}$ is in the range of 10 A, all the evaluated EPC transistors can achieve ZVS for a large load range. EPC2031 is selected for its lower conduction loss.

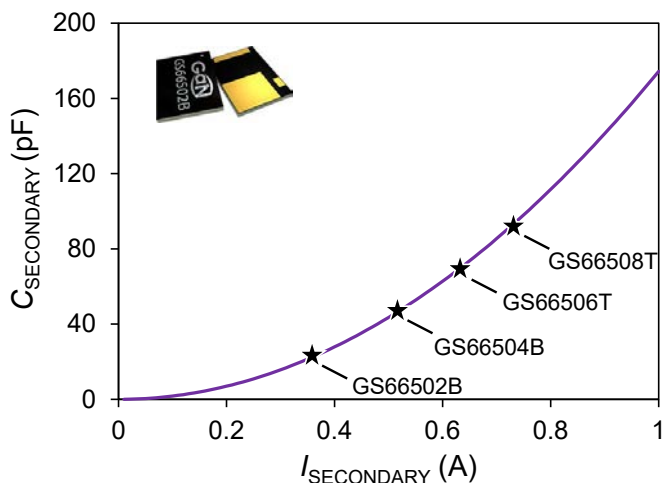


Fig. 5 Selection criterion for HV GaN transistors. GS66502B is selected for its minimum C_{OSS} , which reduces secondary-side switching loss at light loads.

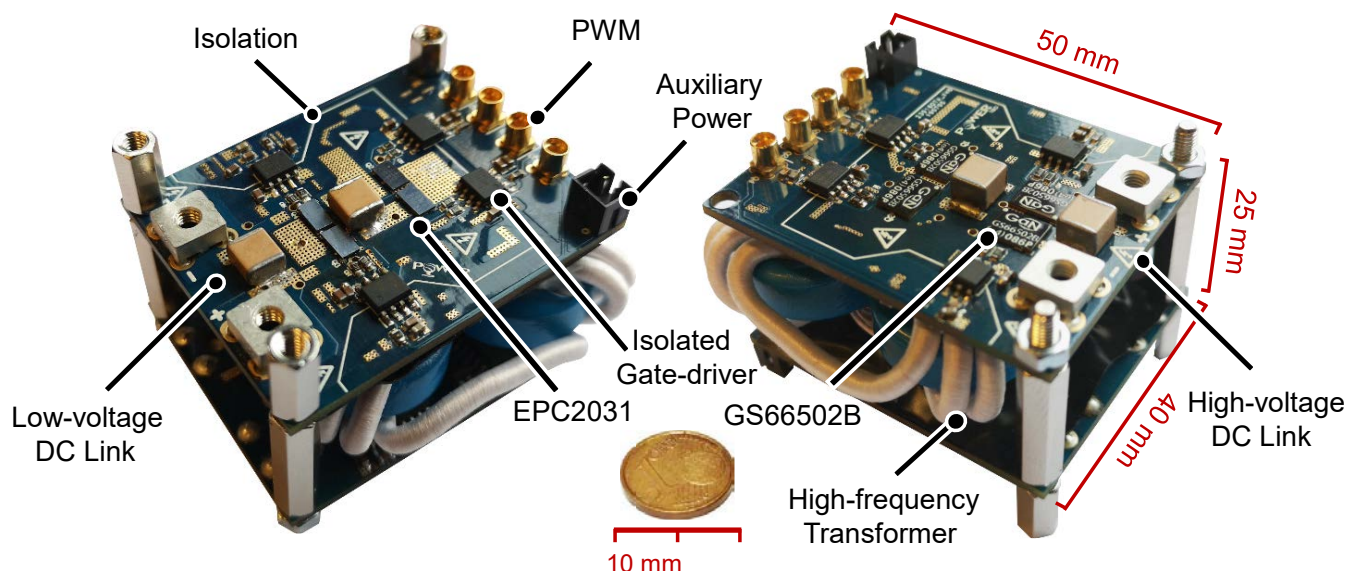


Fig. 6 DAB converter view from primary (Left) and secondary (right) sides, with a 1-cent euro coin. The drive and control stages are galvanically isolated from power stage. The quasi-planar HF transformer is sandwiched between primary and secondary full-bridges, enabling high power density.

The nominal current of the secondary side is in the order of 1 A, and devices with extremely low $R_{DS(ON)}$ (e.g. GS66508T) lead to large switching loss at light loads. Therefore, we selected GS66502B transistor with the lowest C_{OSS} .

4 Converter Design

Power-transfer in DAB when a single phase-shift modulation is used can be expressed as

$$P = \frac{V_{IN}V_{OUT}\left(\frac{\varphi}{\pi}\right)\left(1-\frac{\varphi}{\pi}\right)}{2nfL_r} \quad (4)$$

in which V_{IN} and V_{OUT} are DC-link voltages for primary and secondary, respectively, φ is the phase shift between them and f is switching frequency. Based on the required maximum transferrable power and L_r value (see Fig. 2b), we selected a switching-frequency of 300 kHz (for a 500-W power transfer). In this frequency, the winding AC resistance of the HF transformer remains significantly low (about 15 m Ω), promising a high efficiency. GaN transistors EPC2031 and GS66502B were used in full-bridge arrangement for primary (LV) and secondary (HV) sides, respectively. Fig. 6 presents the DAB converter with the transformer sandwiched between the two full-bridges. The design was realized with minimum parasitic inductance for gate-drive and power loops, in a four-layer printed-circuit board (PCB) design. Isolated gate drivers (SI8271) are separately supplied with 5-V isolated DC/DC converters (ADUM5000) on the bottom layer.

Fig. 6 shows the compact converter dimensions (50 x 40 x 25 mm). This small size is to a great extent thanks to the utilization of the leakage inductance of the quasi-planar HF transformer for power transfer and ZVS, without the need to add external inductors. In fact, the design of high-quality inductors at high frequencies is extremely challenging [13]. The transformer provides galvanic isolation between primary and secondary which is of great significance to many applications including EV charging. All control and drive signals are galvanically isolated from the power circuit, enabling a high level of safety and scalability, as many DABs could be employed to operate in parallel. TMS320F28379D DSP provided the PWM signals for driving the FETs, using shielded cables with MMCX connectors. Dead-time values of 20 ns and 40 ns were applied for primary and secondary full-bridges, respectively.

5 Experimental Results

The converter was operated at 300 kHz, with single-phase-shift modulation and at DC-link voltages of 33 V (primary) and 400 V (secondary). Transformer primary voltage waveform ($V_{PRIMARY}$) is shown in Fig. 7, where all the primary FETs achieve a soft switching transition (ZVS). At the same input-output voltage condition, the efficiency of the converter versus power is measured and shown in Fig. 8. The converter achieved a peak efficiency of 97.4% and an efficiency greater than 91% for a large sweep of power from 100 W to almost 500 W.

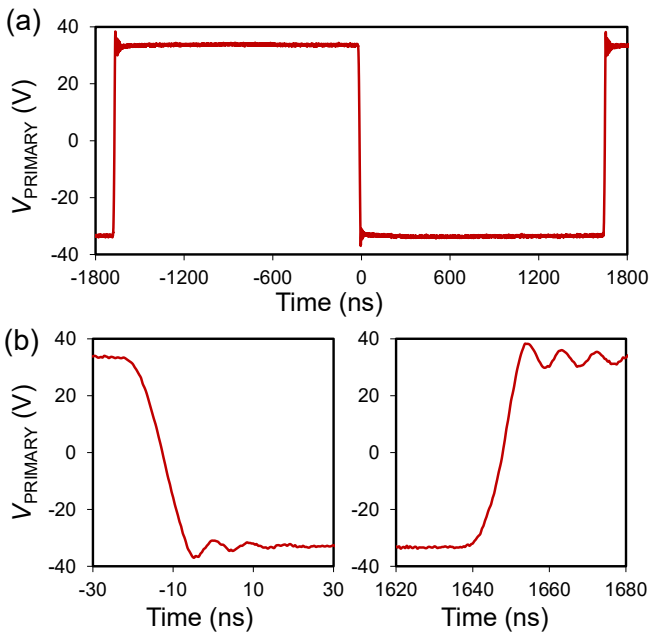


Fig. 7 DAB operating at 200 W with 12-time step-up. (a) Transformer primary voltage together with its (b) falling and rising transitions measured with TPP1000 1-GHz voltage probe. FETs achieve ZVS.

The efficiency could be increased further by employing more sophisticated modulation techniques. However, a proper design strategy and use of the novel HF transformer guaranteed soft-switching as well as small core and winding losses, which resulted in a high efficiency even by using the simplest modulation even at such large voltage step-up. The peak efficiency versus power density is benchmarked for state-of-the-art DC-DC converters in Fig. 9 with their reported step-

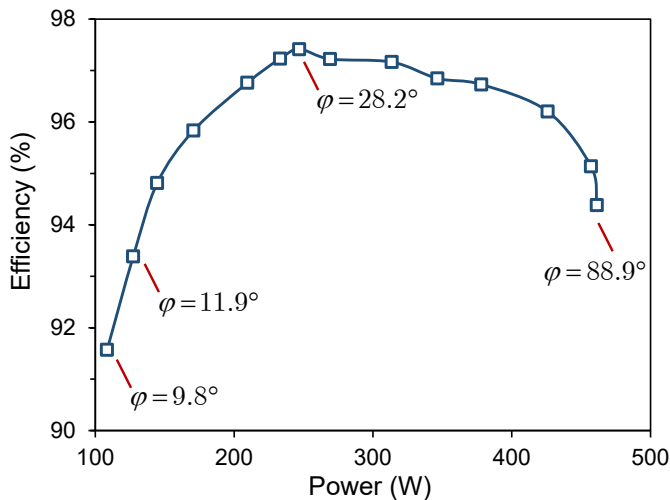


Fig. 8 DAB Efficiency versus power while operating at 300 kHz and boosting 33 V at the input to 400 V at the output. Adjusting a single-phase-shift value, ϕ , simply controls the power-transfer. The converter achieved a peak efficiency of 97.4% with an overall efficiency greater than 91%.

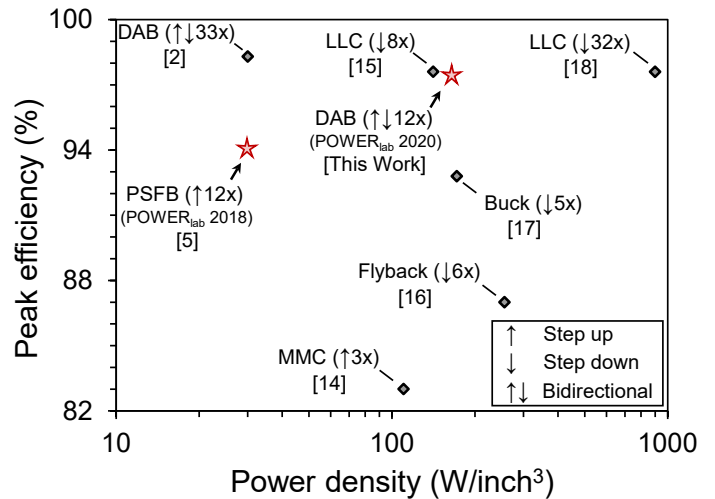


Fig. 9 Benchmarking HF DC-DC converters based on peak efficiency versus power density. This work achieves extremely high efficiency and its power density outperforms state-of-the-art bidirectional power converters.

up/down values [2], [5], [14]–[18], where the proposed DAB design and a previous work [5] are marked with star symbol.

6 Gain versus Power-Transfer Characteristic and Applications

DAB power capability has a dependency on input and output voltages based on (4). This dependency is shown in Fig. 10 for the designed DAB when the output voltage is fixed at 400 V and the input voltage is swept from 30 V to 40 V, with 2-V steps. The power-transfer can be controlled in both directions using a single parameter, ϕ . Its high efficiency and galvanic isolation, makes the DAB a unique topology to serve as a regulated DC transformer for future DC micro-grids in distribution-level. For example, it can be employed to harvest the maximum power from a PV panel with wide voltage/power variations (see Fig. 10).

To achieve ZVS, the voltage gain (G) of the full-bridge DAB should satisfy the inequality [4]

$$n \left(1 - 2 \frac{\phi}{\pi} \right) < G < \frac{n}{1 - 2 \frac{\phi}{\pi}} \quad (5).$$

An overview of ZVS operation in DAB can be obtained by combining the gain limits of (5) with power-transfer characteristic as formulated in (4). The result is a gain versus power-transfer plane, as illustrated in Fig. 11. One can use this characteristic to design a control scheme with the strategy of maintaining ZVS (to minimize system loss, lower the risk of device thermal runaway and increase reliability). Furthermore, it provides insights on evaluating the behavior of DAB under

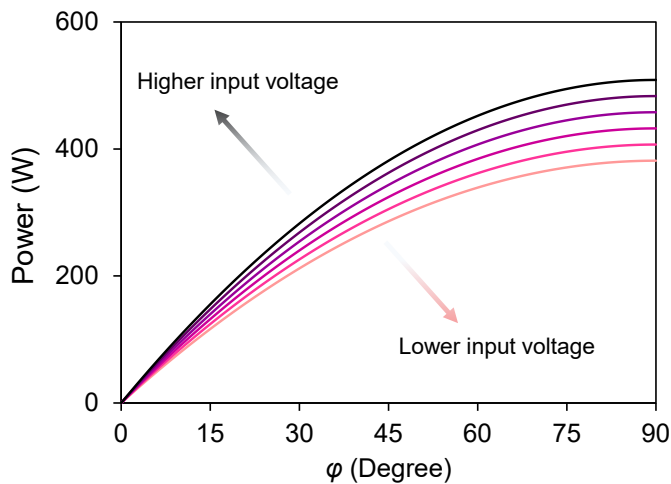


Fig. 10 Dependence of power-transfer capability in DAB on the input voltage, when the output voltage is at a fixed value of 400 V. DAB converter with its straight-forward regulation, can be regarded as DC transformer, capable of harvesting maximum power from renewables sources such as PVs with wide voltage/power variations, enabling their connection to future DC micro-grids.

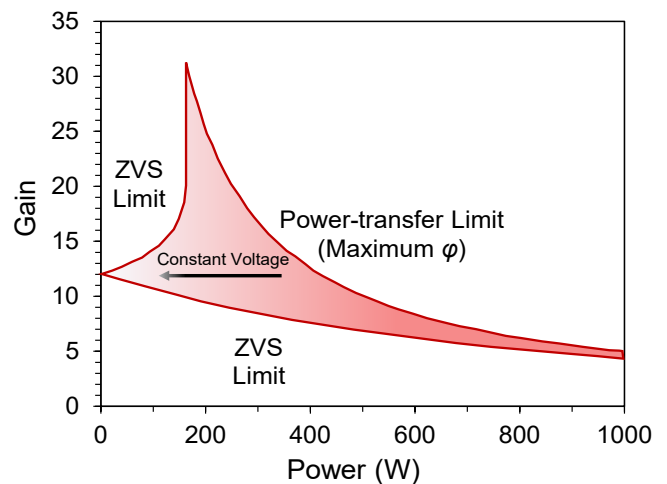


Fig. 11 Gain versus power-transfer characteristic of DAB. The shaded region indicates ZVS operation. The arrow indicates the CV mode in Li-Ion battery-charging process, where the transferred power to the battery gradually decreases over time. HF DAB is an optimum choice for such applications (i.e. on-board EV chargers) thanks to its high power density, excellent efficiency and simple regulation.

different operating conditions. Especially it is critical to maintain soft-switching in high-frequency converters, as the high switching frequency exacerbates the losses occurred due to hard-switching. For instance, a very common application for DC-DC converters is for battery charging. In the case of Li-Ion batteries, two intervals exist; First, a constant-current (CC) mode in which the current is fixed, and the voltage over battery increases close to the nominal voltage. Then the constant-voltage (CV) mode begins, during which the battery voltage is constant and the current (equivalently the power) fed to the battery decreases gradually over time. In this mode, the efficiency of typical converters drops at light loads. However, as the gain versus power-transfer characteristic of Fig. 11 shows, DAB can operate efficiently within its ZVS boundaries, with the lowest thermal stress on transistors. The HF DAB with its high power density, excellent efficiency and simple modulation is of great importance to several applications, including on-board EV charging and renewable energy harvesting in DC micro-grids.

7 Conclusion

In this paper, a high-frequency DAB with state-of-the-art efficiency and power-density (97.4% at 10 kW/l or 164 W/inch³) was demonstrated. A high-frequency quasi-planar

matrix transformer was proposed as the main component responsible for step-up/down and soft-switching. GaN transistors allowed operation at a high switching frequency of 300 kHz. At 12-time step-up/down, the peak efficiency reached 97.4% and remained greater than 91% for a wide range of power from 500 W down to 100 W. Thanks to the quasi-planar design of the transformer and by using its own leakage inductance for power-transfer and achieving ZVS, the power-density reached up to 10 kW/l. We discussed in details the different aspects of the high-frequency DAB converter design, including transformer design and measurement as well as transistor selection criterion. The gain versus power-transfer characteristic was derived and its importance in operation of DAB as a control strategy for achieving ZVS over wide gain and power conditions was explained. The HF DAB is of great significance to many low-voltage DC (LVDC) applications such as on-board battery chargers for electric vehicles, telecommunications, avionics, wind and solar generation systems. Furthermore, thanks to the bidirectional power-transfer capability and straightforward modulation, it could be employed as a DC transformer for future DC distribution systems and microgrids.

8 References:

- [1] S. P. Engel, M. Stieneker, N. Soltau, S. Rabiee, H. Stagge, and R. W. De Doncker, "Comparison of the Modular Multilevel DC Converter and the Dual-Active Bridge Converter for Power Conversion in HVDC and MVDC Grids," *IEEE Trans. Power Electron.*, vol. 30, no. 1, pp. 124–137, Jan. 2015, doi: 10.1109/TPEL.2014.2310656.
- [2] F. Xue, R. Yu, and A. Q. Huang, "A 98.3% Efficient GaN Isolated Bidirectional DC–DC Converter for DC Microgrid Energy Storage System Applications," *IEEE Transactions on Industrial Electronics*, vol. 64, no. 11, pp. 9094–9103, Nov. 2017, doi: 10.1109/TIE.2017.2686307.
- [3] F. Krismer, "Modeling and Optimization of Bidirectional Dual Active Bridge DC-DC Converter Topologies," ETHZ, 2010.
- [4] A. Jafari, M. Samizadeh Nikoo, F. Karakaya, and E. Matioli, "Enhanced DAB for Efficiency Preservation using Adjustable-Tap High-Frequency Transformer," *IEEE Trans. Power Electron.*, pp. 1–1, 2019, doi: 10.1109/TPEL.2019.2958632.
- [5] A. Jafari and E. Matioli, "High Step-Up High-Frequency Zero-Voltage Switched GaN-Based Single-Stage Isolated DC-DC Converter for PV Integration and Future DC Grids," PCIM Europe 2018; International Exhibition and Conference for Power Electronics, Intelligent Motion, Renewable Energy and Energy Management, Nuremberg, Germany, 2018, pp. 1-6.
- [6] M. Samizadeh Nikoo, A. Jafari, N. Perera, and E. Matioli, "New Insights on Output Capacitance Losses in Wide-Band-Gap Transistors," *IEEE Trans. Power Electron.*, pp. 1–1, 2019, doi: 10.1109/TPEL.2019.2958000.
- [7] M. Samizadeh Nikoo, A. Jafari, N. Perera, and E. Matioli, "Measurement of Large-Signal COSS and COSS Losses of Transistors Based on Nonlinear Resonance," *IEEE Trans. Power Electron.*, vol. 35, no. 3, pp. 2242–2246, Mar. 2020, doi: 10.1109/TPEL.2019.2938922.
- [8] B. Zhao, Q. Song, W. Liu, and Y. Sun, "Overview of Dual-Active-Bridge Isolated Bidirectional DC–DC Converter for High-Frequency-Link Power-Conversion System," *IEEE Transactions on Power Electronics*, vol. 29, no. 8, pp. 4091–4106, Aug. 2014, doi: 10.1109/TPEL.2013.2289913.
- [9] W. Choi, K.-M. Rho, and B.-H. Cho, "Fundamental Duty Modulation of Dual-Active-Bridge Converter for Wide-Range Operation," *IEEE Trans. Power Electron.*, vol. 31, no. 6, pp. 4048–4064, Jun. 2016, doi: 10.1109/TPEL.2015.2474135.
- [10] N. Hou and Y. Li, "Overview and Comparison of Modulation and Control Strategies for Non-Resonant Single-Phase Dual-Active-Bridge dc-dc Converter," *IEEE Trans. Power Electron.*, pp. 1–1, 2019, doi: 10.1109/TPEL.2019.2927930.
- [11] M. Yaqoob, K. H. Loo, and Y. M. Lai, "Extension of Soft-Switching Region of Dual-Active-Bridge Converter by a Tunable Resonant Tank," *IEEE Trans. Power Electron.*, vol. 32, no. 12, pp. 9093–9104, Dec. 2017, doi: 10.1109/TPEL.2017.2654505.
- [12] H. Chen, K. Sabi, H. Kim, T. Harada, R. Erickson, and D. Maksimovic, "A 98.7% Efficient Composite Converter Architecture With Application-Tailored Efficiency Characteristic," *IEEE Trans. Power Electron.*, vol. 31, no. 1, pp. 101–110, Jan. 2016, doi: 10.1109/TPEL.2015.2398429.
- [13] R. S. Yang, A. J. Hanson, B. A. Reese, C. R. Sullivan, and D. J. Perreault, "A Low-Loss Inductor Structure and Design Guidelines for High-Frequency Applications," *IEEE Trans. Power Electron.*, vol. 34, no. 10, pp. 9993–10005, Oct. 2019, doi: 10.1109/TPEL.2019.2892397.
- [14] A. Barchowsky, J. P. Kozak, B. M. Grainger, W. E. Stanchina, and G. F. Reed, "A GaN-based modular multilevel DC-DC converter for high-density anode discharge power modules," in *2017 IEEE Aerospace Conference*, Big Sky, MT, USA, 2017, pp. 1–10, doi: 10.1109/AERO.2017.7943768.
- [15] R. Chen and S. Yu, "A high-efficiency high-power-density 1MHz LLC converter with GaN devices and integrated transformer," in *2018 IEEE Applied Power Electronics Conference and Exposition (APEC)*, San Antonio, TX, USA, 2018, pp. 791–796, doi: 10.1109/APEC.2018.8341102.
- [16] Z. Zhang, K. D. T. Ngo, and J. L. Nilles, "A 30-W flyback converter operating at 5 MHz," in *2014 IEEE Applied Power Electronics Conference and Exposition - APEC 2014*,

- Fort Worth, TX, USA, 2014, pp. 1415–1421, doi: 10.1109/APEC.2014.6803492.
- [17] X. Zhang *et al.*, “A GaN transistor based 90W AC/DC adapter with a buck-PFC stage and an isolated Quasi-switched-capacitor DC/DC stage,” in *2014 IEEE Applied Power Electronics Conference and Exposition - APEC 2014*, Fort Worth, TX, USA, 2014, pp. 109–116, doi: 10.1109/APEC.2014.6803296.
- [18] C. Fei, F. C. Lee, and Q. Li, “High-efficiency high-power-density 380V/12V DC/DC converter with a novel matrix transformer,” in *2017 IEEE Applied Power Electronics Conference and Exposition (APEC)*, Tampa, FL, USA, 2017, pp. 2428–2435, doi: 10.1109/APEC.2017.7931039.